HHS Public Access

Author manuscript

Toxicol Appl Pharmacol. Author manuscript; available in PMC 2022 April 30.

Published in final edited form as:

Toxicol Appl Pharmacol. 2022 February 01; 436: 115884. doi:10.1016/j.taap.2022.115884.

Arsenic activates STAT3 signaling during the transformation of the human bronchial epithelial cells

Bandar Almutairy[a,d], **Yao Fu**[b], **Zhuoyue Bi**[b], **Wenxuan Zhang**[b], **Priya Wadgaonkar**[a], **Yiran Qiu**[b], **Chitra Thakur**[b,c], **Fei Chen**[b,c,*]

[a]Department of Pharmaceutical Sciences, Eugene Applebaum College of Pharmacy and Health Sciences, Wayne State University, 259 Mack Avenue, Detroit, MI 48201, USA

[b]Stony Brook Cancer Center, Renaissance School of Medicine, Stony Brook University, Lauterbur Drive, Stony Brook, NY 11794, USA

[c]Department of Pathology, Renaissance School of Medicine, Stony Brook University, 101 Nicolls Road, Stony Brook, NY 11794, USA

[d]College of Pharmacy, Al-Dawadmi Campus, Shaqra University, P.O.Box 11961, Riyadh, Saudi Arabia

Abstract

Arsenic (As^{3+}), a metalloid abundant in environment, is classified as a group I carcinogen associated with several common human cancers, including cancers in lung, skin, bladder, liver, and prostate (Wei et al., 2019). The mechanisms of As^{3+}-induced carcinogenesis had been extensively studied, and different mechanisms might be involved in different types of cancer (Wei et al., 2019). Recent studies showed that exposure to a high dose of arsenic is able to induce lung cancer. Meanwhile, prolonged exposure to a low concentration of arsenic can increase the risk of lung cancer also (Liao et al., 2009; Fernández et al., 2012). Emerging evidence indicated that prolonged exposure to arsenic promotes malignant transformation and some of the transformed cells have cancer-stem-like properties (Ngalame et al., 2014). In the present report, we revealed that exposure to As^{3+} for short time period inhibited tyrosine-705 phosphorylation of signal transducer and activator of transcription 3 ($pSTAT3^{Y705}$) and induced Src homology region 2 domain-containing phosphatase-1 (SHP-1) in bronchial epithelial cell line, BEAS-2B. In addition, we found that long term exposure of the cells to As^{3+} activates phosphorylation of STAT3 at serine 727 ($pSTAT3^{S727}$) as well as $pSTAT3^{Y705}$. Moreover, As^{3+} is able to induce the expression of miRNA-21 (miR-21)

*Corresponding author at: Stony Brook Cancer Center, Department of Pathology, Renaissance School of Medicine, Stony Brook University, Lauterbur Drive, Stony Brook, NY 11794, USA., Fei.Chen.1@stonybrook.edu (F. Chen).

Credit author statement

- Bandar Almutairy performed experiments, data curation and made the original draft of the manuscript.
- Yao Fu, Zhuoyue Bi, Wenxuan Zhang, Priya Wadgaonkar, Yiran Qiu, and Chitra Thakur provided assistance, shared resources and did some of the experiments presented in this manuscript.
- Fei Chen conceptualized the study, designed the experiments and made the final version of this manuscript.

Declaration of Competing Interest

The authors declare no conflict of interest to be revealed.

and decrease the expression of PDCD4. Taken together, our data suggest that activation of STAT3 and induction of miR-21 are important contributing factors to the reduced expression of PDCD4, which may play significant role in As^{3+}-induced transformation of BEAS-2B cells.

Keywords

Arsenic; STAT3; miR-21; PDCD4; Transformation

1. Introduction

Arsenic exposure, mainly in drinking water, is a significant health issue affecting >140 million people in more than 70 countries (Mukherjee et al., 2006). The Environmental Protection Agency (USEPA) and the World Health Organization (WHO) determine the maximum contaminant level of arsenic in drinking water is ten ppb (10 μg/L). In some areas of the USA, the arsenic level in ground water is between 680 and 1880 g/L (~9 to 25 μM), exceeding the maximum contaminant level (Camacho et al., 2011; Ayotte et al., 2017). Worldwide, arsenic contamination in drinking water, ground water or other types of water bodies is still a major health concern for the public. For example, the most recent survey by Osuna-Martinez et al. (Osuna-Martinez et al., 2021) showed that the arsenic level reaches 8684 ppb (~121 μM) and 16,000 ppb (~222 μM) in the continental surficial water and groundwater, respectively, of San Luis Potosi. Such levels of arsenic is far beyond the maximun arsenic level (100–200 μM) used in many short-term experiments addressing the signaling activating or totoxicity property of arsenic. Despite the fact that several studies showed the importance of arsenic in inducing malignant transformation of normal cells, it is not fully understood how arsenic induces transformation as well as the generation of the cancer stem-like cells (CSCs). CSCs are a small group of tumor cells that have some characteristics of stem cells, such as the ability of self-renewing, differentiating into tumor cells with different surface markers and tumorigenicity (Yu et al., 2012). CSCs can be derivated from cancer cells due to dedifferentiation or from normal stem cells due to inhibition of differentiation. CSCs play a significant role in cancer heterogeneity, progression, metastasis, and therapeutic resistance (Chen et al., 2016). Most CSCs showed overexpression of central stemness circuit genes, including Sox2, c-Myc, Oct4, Nanog, and Wnt, which are essential for self-renewal and pluripotency. Additionally, some CSCs found in solid and non-solid tumors express surface protein markers such as CD133, nestin, and CD44 (Yang et al., 2020).

C-Jun N-terminal kinases (JNK) is a key kinase involved in regulating various aspects of the cells and plays significant roles in cancer progression by controlling a broad spectrum of signaling pathways in response to stress and oncogenic signals. JNK has a potential role in CSCs in vitro and in vivo. Crosstalk has been found between JNK activation and WG/DPP or JAK/STAT signaling in different CSCs models (Chen, 2012). Our previous studies showed that in human bronchial epithelial cell BEAS-2B, the signaling is driven from JNK to STAT3 and eventually to AKT in As^{3+} treated cells (Liu et al., 2012). Phosphorylation of STAT3 at tyrosine705 residue ($pSTAT3^{Y705}$) is the known activation of STAT3 in response to cytokines and JAK activation. However, under some cellular

stress conditions, STAT3 is phosphorylated at serine residue 727 (pSTAT^{S727}) and increases cell proliferation, invasion and tumorigenesis of the cancer cells. In BEAS-2B cells, we had shown that short term treatment of the cells with arsenic induces pSTAT3^{S727} but represses pSTAT3^{Y705}. Meanwhile, inhibition of JNK by either JNK inhibitor or JNK siRNA prevented phosphorylation of pSTAT3^{S727} with no effect on pSTAT3^{Y705}, suggesting that JNK regulates pSTAT3^{S727} but not pSTAT3^{Y705} (Liu et al., 2012; Chen et al., 2013). It had been proposed that pSTAT3^{S727} but not pSTAT3^{Y705} is mainly needed for the self-renewal of stem cells and CSCs. Moreover, pSTAT3^{S727} can suppress mitochondrial gene expression during oncogene Ras-induced transformation (Sancho et al., 2009). Studies showed that both JNK and STAT3 could regulate various miRNA expression in different cancer cells. STAT3 directly activates miRNA-21 (miR-21) and miR-181b-1 via PTEN and CYLD as the epigenetic switch from non-transformed to transformed cells (Iliopoulos et al., 2010). Also, As^{3+} has been shown to trigger and shift miRNA expression in different cancer models. For instance, As^{3+} can induce miR-143 in prostate cancer stem cells with multiple cancer characteristics (Ngalame et al., 2016). Mature miRNAs such as miR-200, miR-302, and miR-369 are able to reprogram the cells to form induced pluripotent stem cells (iPSCs) (Miyoshi et al., 2011).

In the present report, we investigated the contribution of STAT3 and miR-21 to As^{3+}-induced transformation of the human bronchial epithelial cell line, BEAS-2B cells, and provided evidence showing that As^{3+} induced JNK, pSTAT3 and miR-21, leading to inhibition of PDCD4 in the As^{3+}-induced transformation and possibly the generation of CSCs. Meanwhile, we showed that short term treatment of the cells with As^{3+} is able to inhibit pSTAT3^{Y705}, possibly through inducing stabilization of SHP-1 protein.

2. Materials and methods

2.1. Cell culture

Because majority of human lung cancers are originated from lung epithelial cells, we selected the human bronchial epithelial cell line BEAS-2B purchased from the American Type Culture Collection (ATCC, Manassas, VA) for the experimentation in this report. BEAS-2B cells were cultured in Dulbecco's modified Eagle's medium (DMEM) with 5% fetal bovine serum (Invitrogen), 1% penicillin-streptomycin and 1% L-Glutamine (Sigma). Cells were maintained in humidified incubator at 37 °C with 5% CO_2. For short term treatment, (3.5×10^5 cells per well) were seeded in 6 wells plates in (DMEM) medium with 5% fetal bovine serum, 1% penicillin-streptomycin and 1% L-glutamine for 48 h. The cells were starved with serum free medium for 12 h, followed by treatment of the cells with various concentration of As^{3+} [arsenic (III) chloride, Sigma-Aldrich, St. Louis, MO] for the indicated times. For long term treatment, BEAS-2B cells were exposure to low concentration of arsenic (0.25 μM) for 24 weeks.

2.2. Western blotting

Cells were lysed in 1 × RIPA buffer (Cell Signaling), supplemented with 1 mM PMSF and protease inhibitor cocktail (Thermo Fisher Scientific). Protein concentrations were determined by Pierce BCA Protein Assay Kit (Thermo Fisher Scientific). Whole cell lysates

(15–20 μg) were separated in sodium dodecyl sulfate-polyacrylamide gel electrophoresis (SDS-PAGE) for 1.5 h at 120 voltages, and then transferred to Polyvinylidene fluoride (PVDF) membranes (Millipore) at room temperature (RT), 200 V, for 1.5 h. The membranes were blocked with 5% nonfat dry milk for 1 h at RT and then probed with primary antibodies at 4 °C overnight. The primary antibodies include anti pSTAT3^{Y705}, pSTAT3^{S727}, STAT3, JNK, pJNK (Th183/Th185), SHP-1, SHP-2, β-actin, PDCD4, SOCS1, and anti-GAPDH (cell signaling). Other primary antibodies purchased from Abcam, including JAK (ab13366), pJAK1 (Y1022/1023, ab138005), pJAK2 (Y1007/1008, ab32101), and SOCS3 (ab78341). After washing with TBST (3 × 10 min), the membranes were incubated with horseradish peroxidase-coupled goat anti-rabbit or -mouse IgG at room temperature for 1 h and washed with TBST (3 × 10 min). Chemiluminescent Substrate (Thermo Fisher Scientific) was used to detect immunoblotting signals. Data are representatives of at least three independent experiments. Micrographs of protein expression and mean percent protein-GAPDH ratio ± (SEM) against treatment. Differences between treatments were analyzed by one-way ANOVA ($p < 0.05$), which is considered significant.

2.3. Real Time-PCR

Total RNA was extracted by TRIzol method and followed by reverse transcription using High-capacity cDNA Reverse Transcription Kits (Applied Biosystems). Each sample contains 2.0 μL 10 × RT Buffer, 0.8 μL 25 × dNTP Mix (100 mM), 2.0 μL 10 × RT Random Primers, 1.0 μL MultiScribe™ Reverse Transcriptase, 1.0 μL RNase Inhibitor, 3.2 μL Nuclease-free H2O), 1 μg total RNA and comparative volume of Nuclease-free water to the total volume of 20 μL. Then, reverse transcription was performed in a thermal cycler according to the protocol (Applied Biosystems). The QPCR mix was prepared for each sample containing: 10 μL Radiant™ Green 2 × qPCR Mix with Fluorescein, 0.8 μL Forward Primer (10 μM), 0.8 μL Reverse Primer (10 μM). The primers are: STAT3 Forward (5′ to 3′): ACCAGCAGTATAGCCGCTTC, Reverse (5′ to 3′): GCCACAATCCGGGCAATCT. SHP-1 Forward (5′ to 3′): TGGCGTGGCAGGA GAACAG. Reverse (5′ to 3′): GCAGTTGGTCACAGAGTAGGGC. PDCD4 5′-GAAGGTTGCTGGATAGGC-3′ (sense): 5′-ATAAACACAGTTCTCCTGGTCATCA-3′ (anti-sense). GAPDH (forward 5′-AGCCACATCGCTCAGACAC-3′: reverse 5′-GCCCAATACGACCAAATCC-3′). About 1 μg template DNA and comparative volume of Nuclease-free water were added to the total volume of 20 μl according to Radiant™ Green Fluorescein qPCR Kit (alkali Scientific Inc.: Fort Lauderdale, FL, USA). The samples were analyzed by QPCR machine (LightCycler® 480 Instrument, from Roche) and GAPDH that was used as a control and relative mRNA expression was calculated using the $2^{(-\Delta\Delta CT)}$ method.

2.4. Real-Time RT-PCR for microRNA

Beas-2B cells (1.0×10^5 cells/well) were seeded in 96 wells plate for 24 h, followed by starvation for 12 h. Then, cells were treated with various concentration of As^{3+} for the indicated times. Cells were washed by cold PBS and incubated in the lysis solution for 8 mins at RT. Then stop solution was added and incubated for 2 mins at RT. Reverse transcription reaction were set up by adding master mix and RT primer for miR21 RNU6B and run the RT on thermal cycle according to the protocol (Taqman MicroRNA Cells-to-CT^{Tm} Kit). The miR-21 was quantified by real time PCR using TaqMan miRNA Assays

(Applied Biosystems) and RNU6B that was used as an endogenous control (Taqman miRNA assays control, cat: 4427975).

2.5. Statistics

The data were analyzed by one-way ANOVA with 95% confidence interval followed by Tukey post-test using GraphPad Prism version 6.00 for Windows (Graph Pad Software, San Diego, CA, USA). Results were obtained from at least triplicate runs of experiments and presented as mean ± SEM, $n = 3$. $P < 0.05$ was considered statistically significant.

3. Results

3.1. Short-term As^{3+} treatment of the cells induces $pSTAT3^{S727}$ and JNK activation but inhibits $pSTAT3^{Y705}$

To test the effect on As^{3+} on the STAT3 and JNK activation, BEAS-2B cells were treated with various concentrations of As^{3+} (0, 0.25, 0.5, 1, 2, 4, 8, 16, 32 μM) for 6 h. As we had reported previously, this treatment induced $pSTAT3^{S727}$, but had no effect on the level of non-phosphorylated STAT3 (Fig. 1A & B). We also examined activation of JNK, a known upstream kinase responsible for $pSTAT^{S727}$, and a concomitant dose-dependent JNK activation was observed (Fig. 1C & D). Interestingly, we found that a high dose of As^{3+}, 32 μM, significantly decreased the level of $pSTAT3^{Y705}$ (Fig. 1E). To further validate that high dose of As^{3+} is inhibitory for $pSTAT3^{Y705}$, we next treated the cell with As^{3+} at concentrations of 0, 10, 20, 40, and 80 μM for 6 h. The results showed that a high dose of As^{3+}, ≥ (20 μM) significantly decreased the level of $pSTAT3^{Y705}$ (Fig. 2A). In contrast, the level of $pSTAT3^{S727}$ is elevated (Fig. 2B), along with an increased activation of JNK as determined by the level of JNK phosphorylation (pJNK, Fig. 2C). We also tested whether the inhibition of $pSTAT3^{Y705}$ by As^{3+} is a result of cell starvation, and found that such an inhibition occurred even in the cell without starvation (Fig. 2D). In addition to the dose-dependent studies above, we also treated the cells with 10 μM As^{3+} for different times and found that the effect of As^{3+} on $pSTAT3^{S727}$ and $pSTAT3^{Y705}$ is in a time-dependent manner. The induction of $pSTAT3^{S727}$ can be detected after 6 h and inhibition of $pSTAT3^{Y705}$ can be noted after 12 h of 10 μM As^{3+} treatment, respectively (Fig. 2E).

3.2. As^{3+} treatment induces JAK1 and JAK2 tyrosine phosphorylation

JAK1 and JAK2 are known upstream kinases for tyrosine phosphorylation of STAT3, and overactivated in some types of cancer. JAKs activate STAT3 through inducing $pSTAT3^{Y705}$ by translating phosphorylation from gp130 domains of JAK receptors to SH2 domain at STAT3 (Iliopoulos et al., 2017). Thus, it will be interesting to know whether the observed decrease of $pSTAT3^{Y705}$ by high concentration of As^{3+} is resulted from inhibition of JAK activation. Interestingly, we found that As^{3+} induced $pJAK1^{Y1022/1023}$ and $pJAK2^{Y1007/1008}$ in a dose-dependent manner, suggesting that the inhibition of $pSTAT3^{Y705}$ by As^{3+} is independent of JAK inhibition (Fig. 3).

3.3. As^{3+} upregulates SHP-1 proteins

The activation of STAT3 is negatively regulated by SOCS family members, including SOCS1 and SOCS3, and by protein tyrosine phosphatases (PTPs), such as SHP-1 and SHP-2 (Iliopoulos et al., 2017). To investigate whether the observed downregulation of $pSTAT3^{Y705}$ by As^{3+} is achieved through these negative regulators of STAT3, we first measured the protein levels of SOCS1, SOCS3 and SHP-2 in the cells treated with different concentrations of As^{3+} for 6 h. No measurable effect of As^{3+} on these proteins was noted (Fig. 4A). We next tested whether As^{3+} regulates SHP-1 (PTPN6), a known PTP that antagonizes $pSTAT3^{Y705}$ through dephosphorylation of Y705 on STAT3. There is a clear dose-dependent induction of SHP-1 by As^{3+} in the BEAS-2B cells (Fig. 4B). This result suggests that the downregulation of $pSTAT3^{Y705}$ by As^{3+} is very likely, at least partially, accomplished through the induction of SHP-1. To confirme this hypothesis further, we also tested the regulation of As^{3+} on $pSTAT3^{Y705}$ and SHP-1 in a previously established transformed cells induced by consecutive As^{3+} treatment for 24 weeks. Although the transformed cells are somewhat resistant to As^{3+}-induced downregulation of $pSTAT3^{Y705}$, there is a clear reverse relationship between $pSTAT3^{Y705}$ and SHP-1 in the cells treated with 80 μM As^{3+} (Fig. 4C).

3.4. As^{3+} decreased the mRNA levels SHP-1, STAT3, and induced the expression of miR-21

Treatment of the cells with As^{3+} increased the protein level of SHP-1 (Fig. 4). To determine whether this regulatory role of As^{3+} on SHP-1 occurs on gene expression level, we next performed real-time PCR to quantify the SHP-1 mRNA in the cells treated with different concentrations of As^{3+} for 6 h and 12 h, respectively. Intriguingly, we found a pronounced inhibition of SHP-1 mRNA by As^{3+} in a roughly dose-dependent manner at two different time point (Fig. 5A & B). A substantial inhibition of SHP-1 mRNA was noted in the cells treated with 5 to 80 μM As^{3+}. Although As^{3+} also marginally inhibits expression of STAT3 mRNA, such an inhibition occurred only in the cells treated with higher concentration of As^{3+}, 40 to 80 μM (Fig. 5C). In contrast, there is a clear dose-dependent induction of miR-21 by As^{3+}, an oncogenic miRNA regulated by STAT3 as we and other had reported previously (Fig. 5D). Thus, these data suggested to us that As^{3+} represses $pSTAT^{Y705}$ by upregulating the SHP-1 protein, but not the SHP-1 mRNA, possibly through stabilizing the SHP-1 protein.

3.5. Sustained activation of STAT3 signaling in the malignantly transformed cells induced by As^{3+}

We had previously established malignantly transformed BEAS-2B cells by consecutive treatment of these cells with 0.25 μM As^{3+} and found some of these transformed cells acquired characteristics of the cancer stem-like cells (CSCs). To determine whether the activation status of STAT3 was altered in these transformed cells, we first measured the levels of $pSTAT3^{Y705}$, $pSTAT3^{S727}$ and SHP-1 in these cells through Western blotting. As depicted in Fig. 6A and B, the transformed cells showed a more than 5-folds and 2-folds increase of $pSTAT3^{Y705}$ and $pSTAT3^{S727}$ relative to the parental BEAS-2B cells, respectively. In contrast, the negative regulator of STAT3, SHP-1, was decreased significantly in the transformed cells (Fig. 6C). Meanwhile, PDCD4, a known target of

STAT3-dependent miR-21, is also decreased considerably in the transformed cells (Fig. 6D). The transformed cells also showed an increased expression of STAT3 mRNA and miR-21 relative to the parental BEAS-2B cells (Fig. 7A & B), whereas the mRNA of SHP-1 was remarkably decreased in the transformed cells (Fig. 7C). A decreased level of PDCD4 mRNA, although marginal, was also noted in the transformed cells. Howevert, such a marginal reduction of PDCD4 mRNA might be not due to transcriptional repression, but rather, the post-transcriptional regulation by miR-21. Accordingly, these results suggest that despite short-term As^{3+} treatment only induces $pSTAT3^{S727}$, both $pSTAT3^{Y705}$ and $pSTAT3^{S727}$ are sustained upregulated in the As^{3+}-induced malignantly transformed cells, which may contribute to the malignant transformation and the formation of the cancer stem-like cells induced by consecutive treatment of the cells with As^{3+}.

4. Discussion

Long-term exposure to environmental arsenic, mainly As^{3+}, via drinking water is the major health concern worldwide. Arsenic is classified as a Group I human carcinogen and has been shown to cause several types of cancers. However, the full mechanisms of arsenic carcinogenesis remain to be fully elucidated, especially the ability of arsenic to transform normal cells and induce the generation of CSCs. In our previous studies, we found that treatment of the BEAS-2B cells with 0.25 μM (~18 ppb) As^{3+} consecutively for 6 months, a procedure to mimic human exposure to environmental arsenic, caused malignant transformation of these cells and the generation of CSCs that featured with increased expression of stemness genes, tumorigenesis, and self-renewal in vitro and in vivo (Chang et al., 2014). STAT3 is an oncogenic transcription factor with pleiotropic effects on cell linage development, carcinogenesis and the stemness of cancer cells or CSCs. One of the mechanisms of STAT3-mediated carcinogenesis and pluripotency/self-renewal of the CSCs is the STAT3-dependent expression of miR-21 that down-regulates several key tumor suppressors, including PDCD4, PTEN and SPRY2 (Chen et al., 2013). Indeed, we had previously demonstrated that As^{3+} is capable of activating STAT3 and inducing miR-21 expression in epithelial cells, which is further validated in the present report (Sun et al., 2014).

Activation of STAT3 is reflected by the phosphorylation of tyrosine705 ($pSTAT3^{Y705}$) and/or serine727 ($pSTAT3^{S727}$) of the STAT3 protein. Emerging evidence suggests that either $pSTAT3^{Y705}$ or $pSTAT3^{S727}$ is important for cell proliferation and malignant transformation. It is interesting to note that As^{3+} at high doses has opposite effect on $pSTAT3^{Y705}$ and $pSTAT3^{S727}$. In response to transient As^{3+} treatment, the major activated form of STAT3 is $pSTAT3^{S727}$. In contrast, As^{3+} appears to be a negative regulator for $pSTAT3^{Y705}$ (Sun et al., 2014). Mitogen activated protein kinase, c-Jun N-terminal kinase (JNK), was believed as an upstream kinase for $pSTAT3^{(S727)}$ (Sun et al., 2014). However, the question that how As^{3+} represses $pSTAT^{Y705}$ was not answered until now. The present data unraveled that As^{3+}-induced accumulation of SHP-1, a PTP that antagonizes $pSTAT3^{Y705}$, may be responsible for the downregulation of $pSTAT^{Y705}$.

At this moment, it is unknown why As^{3+} increases SHP-1 protein but decreases SHP-1 mRNA in a short-term treatment of the cells (Figs. 4 & 5). In the transformed cells

induced by long-term As^{3+} treatment, however, both protein and mRNA of SHP-1 were decreased, which correlated to a substantial upregulation of $pSTAT3^{Y705}$ in the transformed cells (Figs. 6 & 7). One possible explanation is that acute As^{3+} treatment may stabilize SHP-1 protein by repressing the protein degradation machinery temporary, leading to a transient downregulation of $pSTAT3^{Y705}$. However, this effect may be reverted by prolonged treatment of the cells with As^{3+} due to sustained inhibition on gene transcription of SHP-1 as reflected by the reduced level of SHP-1 mRNA (Fig. 5A & B). In combination of upregulation of $pSTAT^{S727}$, activation of JAK1 and JAK2 (Fig. 3), adaptation of the cells, and cell colony repopulation, long-term treatment of the cells with As^{3+} will finally exhibit overall repressive role on both SHP-1 mRNA and protein, and the consequent elevation of both $pSTAT3^{Y705}$ and $pSTAT3^{S727}$ that promote malignant transformation of the cells and the generation of CSCs (Fig. 8).

PDCD4 has long been viewed as a tumor suppressor that inhibits tumor cell proliferation, invasion and metastasis, although no genetic mutation of the Pdcd4 gene had been identified in cancers (Matsuhashi et al., 2019). PDCD4 can function as an inhibitor for both cap-dependent and IRES-dependent translation initiation of the proteins through physical interaction with eIF4B and the specific secondary structure of mRNAs, respectively. Meanwhile, PDCD4 is also capable of interrupting JNK-dependent activation of AP-1 transcription factor by preventing phosphorylation of c-Jun. PDCD4 is one of the targets of the oncogenic miRNA, miR-21 (Chen et al., 2013). Thus, the signaling axis of JNK and STAT3 activation that linked to miR-21 overexpression may be critically involved in the downregulation of PDCD4 and several other tumor suppressor-like protein during As^{3+}-induced malignant transformation and the formation of the CSCs.

It is interesting to note that in addition to the direct regulation of STAT3 on miR-21, the upstream kinase of STAT3, JNK, had also been unraveled as a transcriptional regulator for miR-21 (Echevarria-Vargas et al., 2014). In cisplatin resistant ovarian cancer cell line, inhibition of JNK diminished expression of pre-miR-21. Moreover, chromatin immunoprecipitation (ChIP) followed by PCR suggested a strong binding of the phosphor-c-Jun to the promoter region of pre-miR-21. The latest genome annotation suggested that the gene of pre-miR-21 is located in the last exon of VMP1 gene. Our recent ChIP-seq analysis revealed multiple enrichment peaks of the As^{3+}-induced transcription factor Nrf2 binding in the genebody of VMP1 (data not shown). Furthermore, in our another ChIP-seq experiment using the control and the As^{3+}-transformed cells, we observed an independent enrichment peak of H3K4me3, an active marker for gene transcription, in the last exon of VMP1 gene where the pre-miR-21 gene is located. Therefore, As^{3+} can elicit multiple signaling pathways, some of which are converged together, that enforce the expression of miR-21 expression.

Taken together, our data presented in this report suggest that the activation of STAT3 by As^{3+} is not in a simple linear manner, but rather a complex and self-reinforcing regulatory circuit converged by several different signaling pathways. Although short-term treatment of the cells with As^{3+} represses $pSTAT3^{Y705}$ due to transient stabilization of SHP-1 protein, inhibition of SHP-1 gene expression, induction of $pSTAT3^{S727}$ and the potent activation of JAK1 and JAK2 predispose the cells with sustained elevation of $pSTAT3^{Y705}$ that enforces

As^{3+}-induced transformation and the generation of CSCs. Our findings in this report, thus, fill the gaps of our knowledge on As^{3+} carcinogenesis and will shed light in therapeutical targets of human cancers associated with environmental As^{3+} exposure.

Acknowledgement

This work was supported by National Institutes of Health (NIH) grants R01 ES031822, R01 ES028335, R01 ES028263, Wayne State University Research Enhancement fund, and Research Start-up fund of the Stony Brook University to FC.

References

Ayotte JD, Medalie L, Qi SL, Backer LC, Nolan BT, 2017. Estimating the high-arsenic domestic-well population in the conterminous United States. Environ. Sci. Technol 51, 12443–12454. [PubMed: 29043784]

Camacho LM, Gutiérrez M, Alarcón-Herrera MT, de Lourdes Villalba M, Deng S, 2011. Occurrence and treatment of arsenic in groundwater and soil in northern Mexico and southwestern USA. Chemosphere 83, 211–225. [PubMed: 21216433]

Chang Q, Chen B, Thakur C, Lu Y, Chen F, 2014. Arsenic-induced sub-lethal stress reprograms human bronchial epithelial cells to CD61- cancer stem cells. Oncotarget 5, 1290–1303. [PubMed: 24675390]

Chen F, 2012. JNK-induced apoptosis, compensatory growth, and cancer stem cells. Cancer Res. 72, 379–386. [PubMed: 22253282]

Chen B, Liu J, Chang Q, Beezhold K, Lu Y, Chen F, 2013. JNK and STAT3 signaling pathways converge on Akt-mediated phosphorylation of EZH2 in bronchial epithelial cells induced by arsenic. Cell Cyde 12, 112–121.

Chen W, Dong J, Haiech J, Kilhoffer M-C, Zeniou M, 2016. Cancer stem cell quiescence and plasticity as major challenges in cancer therapy. In: Stem Cells International 2016.

Echevarria-Vargas IM, Valiyeva F, Vivas-Mejia PE, 2014. Upregulation of miR-21 in cisplatin resistant ovarian cancer via JNK-1/c-Jun pathway. PLoS One 9, e97094. [PubMed: 24865582]

Fernández MI, López JF, Vivaldi B, Coz F, 2012. Long-term impact of arsenic in drinking water on bladder cancer health care and mortality rates 20 years after end of exposure. J. Urol 187, 856–861. [PubMed: 22248521]

Iliopoulos D, Jaeger SA, Hirsch HA, Bulyk ML, Struhl K, 2010. STAT3 activation of miR-21 and miR-181b-1 via PTEN and CYLD are part of the epigenetic switch linking inflammation to cancer. Mol. Cell 39, 493–506. [PubMed: 20797623]

Iliopoulos D, Hirsch HA, Struhl K, Banerjee K, Resat H, Ji Z, He L, Regev A, Struhl K, Bersimbaev R, Pulliero A, Bulgakova O, Asia K, Aripova A,Izzotti A, Iliopoulos D, Jaeger SA, Hirsch HA, Bulyk ML, Struhl K, Yuan J, Zhang F, Niu R, Huynh J, Etemadi N, Hollande F, Ernst M, Buchert M, 2017. Constitutive activation of STAT3 in breast cancer cells: a review. Int. J. Cancer 39, 1–10.

Liao C-M, Shen H-H, Chen C-L, Hsu L-I, Lin T-L, Chen S-C, Chen C-J, 2009. Risk assessment of arsenic-induced internal cancer at long-term low dose exposure. J. Hazard. Mater 165, 652–663. [PubMed: 19062162]

Liu J, Chen B, Lu Y, Guan Y, Chen F, 2012. JNK-dependent Stat3 phosphorylation contributes to Akt activation in response to arsenic exposure. Toxicol. Sci 129, 363–371. [PubMed: 22696236]

Matsuhashi S, Manirujjaman M, Hamajima H, Ozaki I, 2019. Control mechanisms of the tumor suppressor PDCD4: expression and functions. Int. J. Mol. Sci 20.

Miyoshi N, Ishii H, Nagano H, Haraguchi N, Dewi DL, Kano Y, Nishikawa S, Tanemura M, Mimori K, Tanaka F, 2011. Reprogramming of mouse and human cells to pluripotency using mature microRNAs. Cell Stem Cell 8, 633–638. [PubMed: 21620789]

Mukherjee A, Sengupta MK, Hossain MA, Ahamed S, Das B, Nayak B, Lodh D, Rahman MM, Chakraborti D, 2006. Arsenic contamination in groundwater: a global perspective with emphasis on the Asian scenario. J. Health Popul. Nutr 142–163. [PubMed: 17195556]

Ngalame NN, Tokar EJ, Person RJ, Waalkes MP, 2014. Silencing KRAS overexpression in arsenic-transformed prostate epithelial and stem cells partially mitigates malignant phenotype. Toxicol. Sci 142, 489–496. [PubMed: 25273566]

Ngalame NN, Makia NL, Waalkes MP, Tokar EJ, 2016. Mitigation of arsenic-induced acquired cancer phenotype in prostate cancer stem cells by miR-143 restoration. Toxicol. Appl. Pharmacol 312, 11–18. [PubMed: 26721309]

Osuna-Martinez CC, Armienta MA, Berges-Tiznado ME, Paez-Osuna F, 2021. Arsenic in waters, soils, sediments, and biota from Mexico: an environmental review. Sci. Total Environ 752, 142062. [PubMed: 33207489]

Sancho R, Nateri AS, De Vinuesa AG, Aguilera C, Nye E, Spencer-Dene B, Behrens A, 2009. JNK signalling modulates intestinal homeostasis and tumourigenesis in mice. EMBO J. 28, 1843–1854. [PubMed: 19521338]

Sun J, Yu M, Lu Y, Thakur C, Chen B, Qiu P, Zhao H, Chen F, 2014.Carcinogenic metalloid arsenic induces expression of mdig oncogene through JNK and STAT3 activation. Cancer Lett. 346, 257–263. [PubMed: 24434654]

Wei S, Zhang H, Tao S, 2019. A review of arsenic exposure and lung cancer. Toxicol. Res. (Camb) 8, 319–327. [PubMed: 31160966]

Yang L, Shi P, Zhao G, Xu J, Peng W, Zhang J, Zhang G, Wang X, Dong Z, Chen F, 2020. Targeting cancer stem cell pathways for cancer therapy. Signal Trans. Target. Therapy 5, 1–35.

Yu Z, Pestell TG, Lisanti MP, Pestell RG, 2012. Cancer stem cells. Int. J. Biochem. Cell Biol 44, 2144–2151. [PubMed: 22981632]

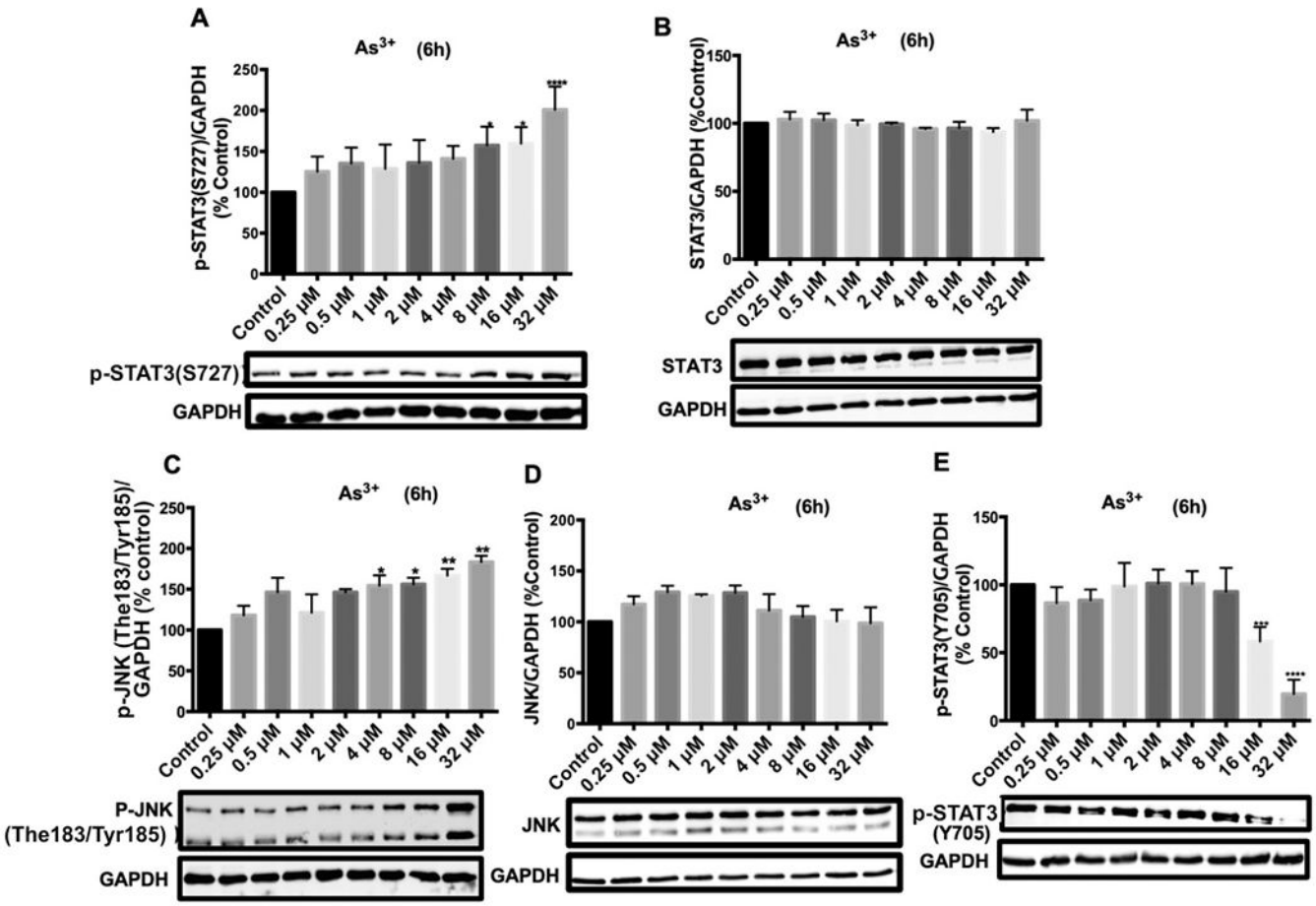

Fig. 1.

Protein expression of pSTAT3^{S727}, STAT3, pJNK$^{Th183/Th185}$, JNK, and pSTAT3^{Y705} in BEAS-2B cells. BEAS-2B cells were treated with various concentrations of As^{3+} for the indicated times followed by Western blotting using the indicated antibodies. The cell lysates were prepared following treatment of the cells with As^{3+} and immunoblotted on PVDF membranes. Membranes were probed for A: pSTAT3^{S727}, B: STAT3, C: pJNK$^{Th183/Th185}$, D: JNK, and E: pSTAT3^{Y705} proteins. Experiments were repeated three times, and the mean percent of protein/GAPDH ratio ± SEM was presented. One way ANOVA was used for statistics analysis *: $p < 0.05$; **: $p < 0.01$; ***: $p < 0.001$, ****: $p < 0.0001$.

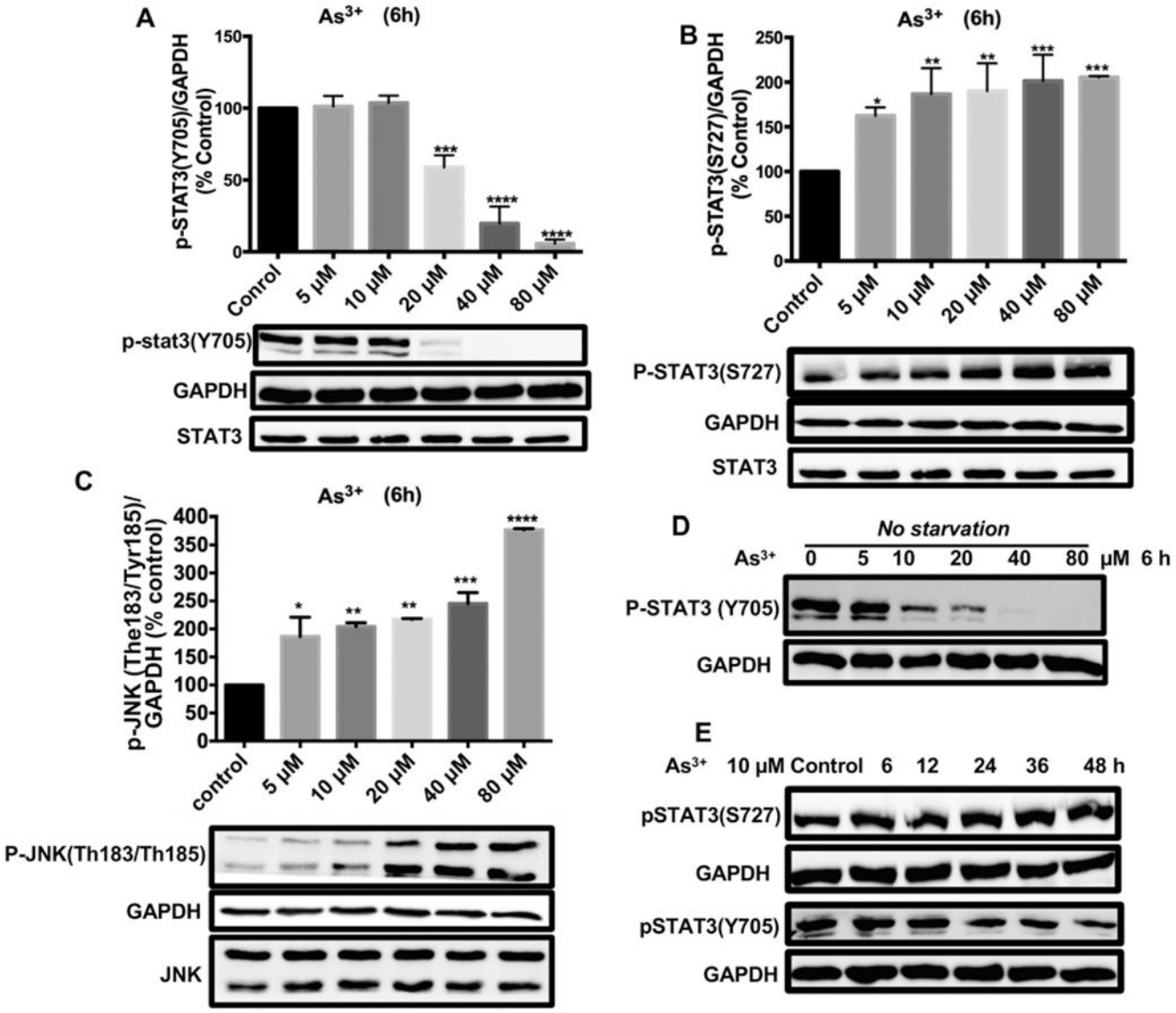

Fig. 2.

Dose and time-dependent effects of As^{3+} on STAT3, and JNK activation. A, B, and C: BEAS-2B cells were starved overnight then treated with various concentrations of As^{3+} (0, 5, 10, 20, 40, 80 μM) for 6 h. D: BEAS-2B cells were treated with various concentrations of As^{3+} for 6 h without starvation. A: $pSTAT3^{Y705}$, B: $pSTAT3^{S727}$, C: $pJNK^{Th183/Th185}$, and D: $pSTAT3^{Y705}$. E: BEAS-2B cells were starved overnight then treated with 10 μM As^{3+} for the indicated times. The levels of $pSTAT3^{S727}$ and $pSTAT3^{Y705}$ proteins expression were confirmed by Western blotting. Experiments were repeated three times, and the mean percent of protein/GAPDH ratio ± SEM was presented. One way ANOVA was used for statistics analysis *: $p < 0.05$; **: $p < 0.01$; ***: $p < 0.001$, ****: $p < 0.0001$.

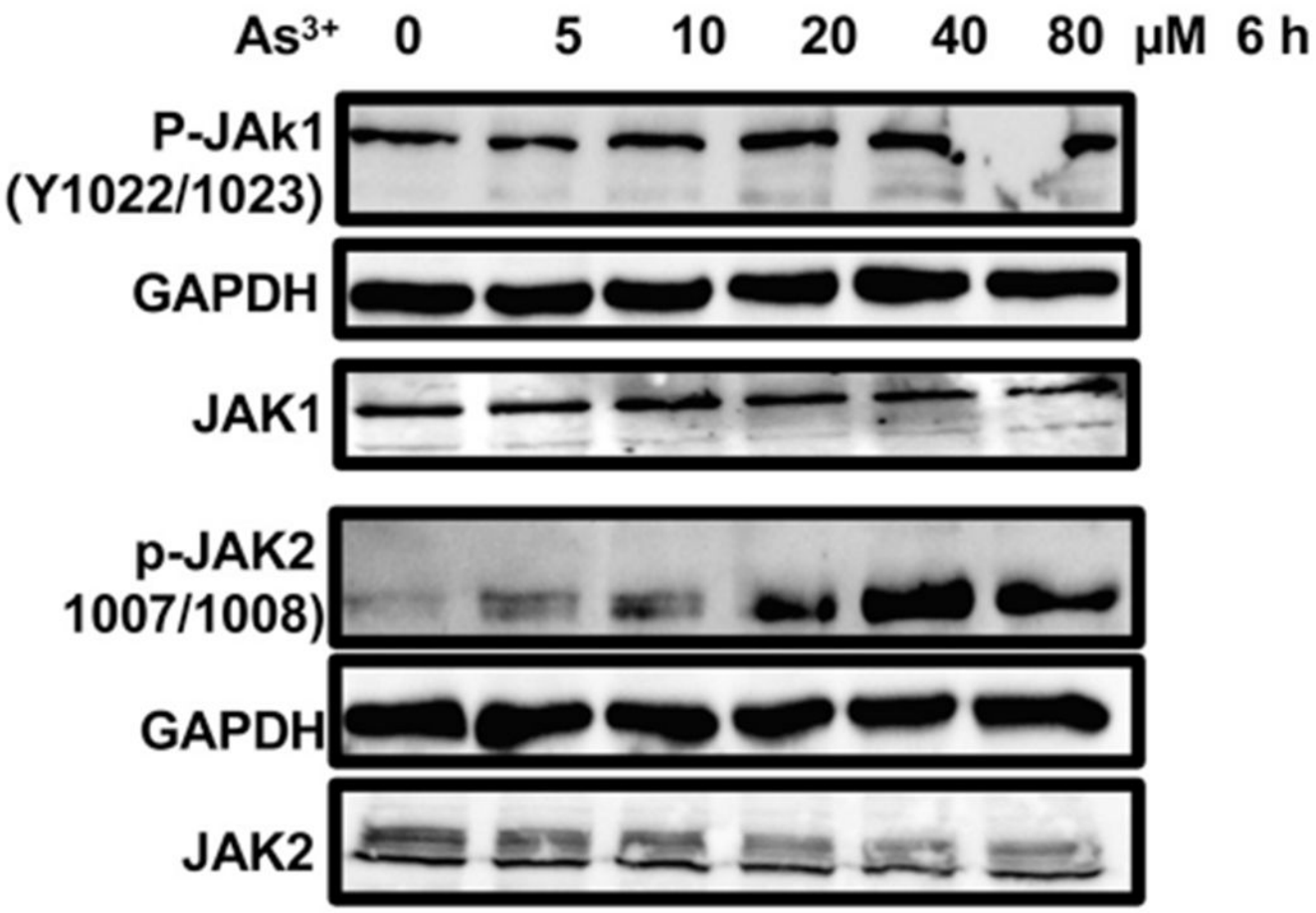

Fig. 3.

As^{3+} activates JAK1 and JAK2: BEAS-2B cells were starved overnight then treated with the indicated concentrations of As^{3+} for 6 h. BEAS-2B cell lysates were prepared following As^{3+} treatment and immunoblotted on PVDF membranes. Membranes were probed with the indicated antibodies. The levels of protein expression were confirmed by Western blotting.

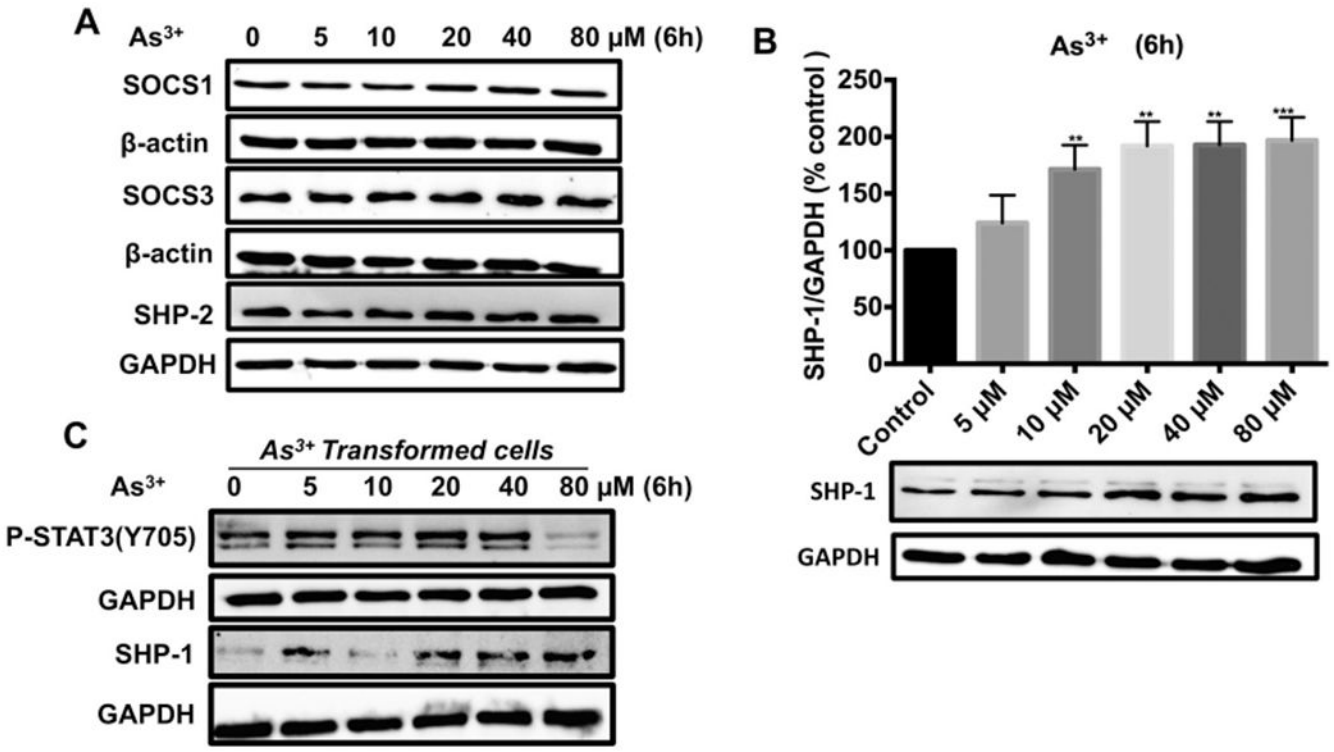

Fig. 4.

The effect of As^{3+} on SOCS1, SOCS3, SHP-1, SHP-2, and $pSTAT3^{Y705}$: A & B: BEAS-2B cells were treated with various concentrations of As^{3+} (0, 5, 10, 20, 40, 80 μM) for 6 h. The levels of SOCS1, SOCS3, SHP-2 (A), and SHP-1 (B) protein expression were confirmed by Western blotting. C: Transformed Cells were treated with various concentrations of As^{3+} (0, 5, 10, 20, 40, 80 μM) for 6 h. The levels of $pSTAT3^{Y705}$, and SHP-1 were determined by western blotting.

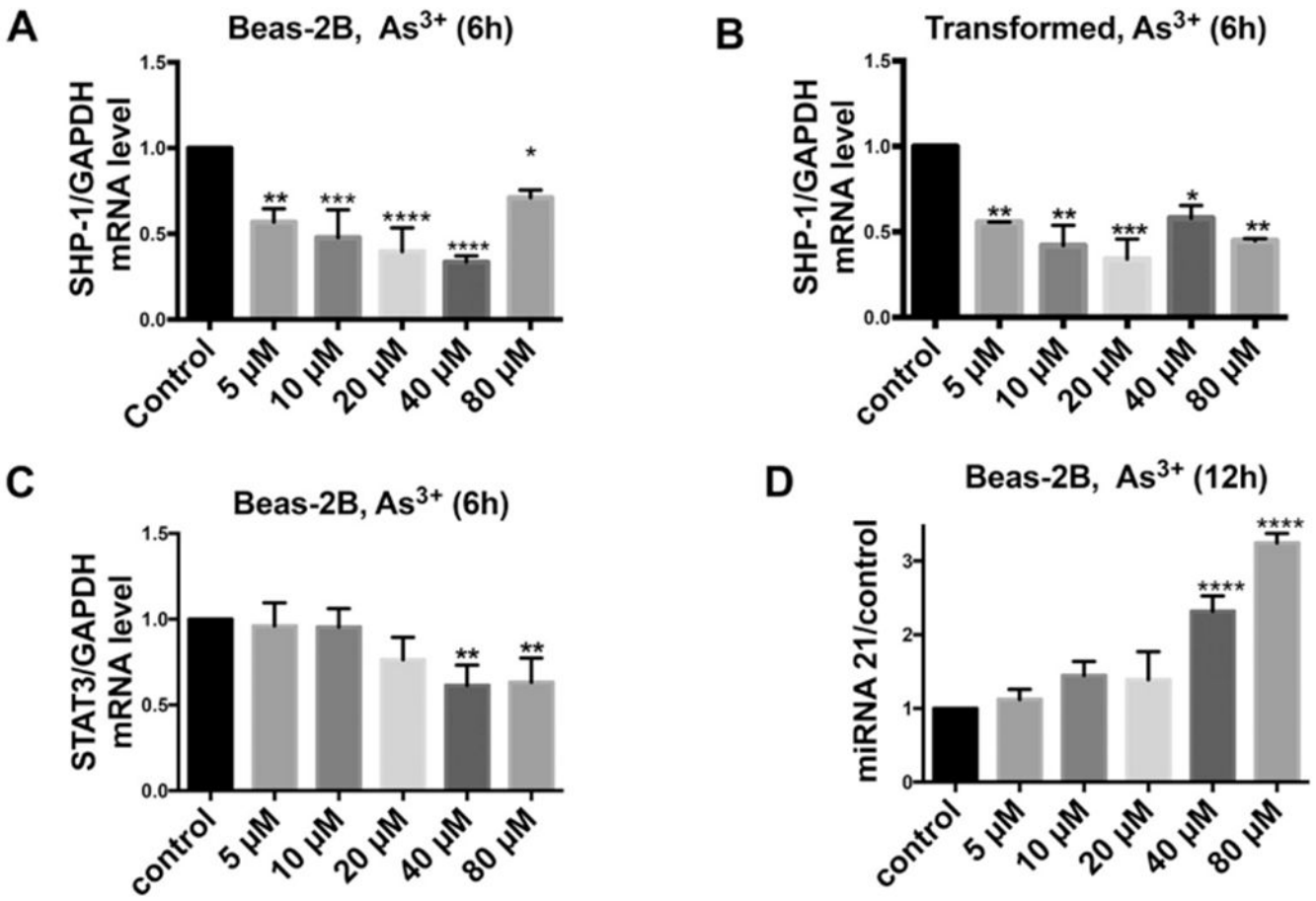

Fig. 5.

Regulatory role of As^{3+} on mRNAs of SHP-1, STAT3, and miR-21. A: BEAS-2B cells were starved overnight then treated with the indicated concentrations of As^{3+} for 6 h. The mRNA level of SHP-1 were determined by real-time PCR. B: Transformed cells starved overnight then treated with As^{3+} as in A. The mRNA level of SHP-1 were determined. C: BEAS-2B cells were starved overnight then treated with As^{3+} as in A. The mRNA level of STAT3 were determined. D: BEAS-2B cells were starved overnight then treated with the indicated concentrations of As^{3+} for 12 h. The level miR-21 were determined by QPCR. All experiments were repeated three times, and the mean percent of mRNA/GAPDH mRNA ratio ± SEM was presented. One way ANOVA was used for statistics analysis. *: p 0.05; **: $p < 0.01$; ***: $p < 0.001$, ****: $p < 0.0001$.

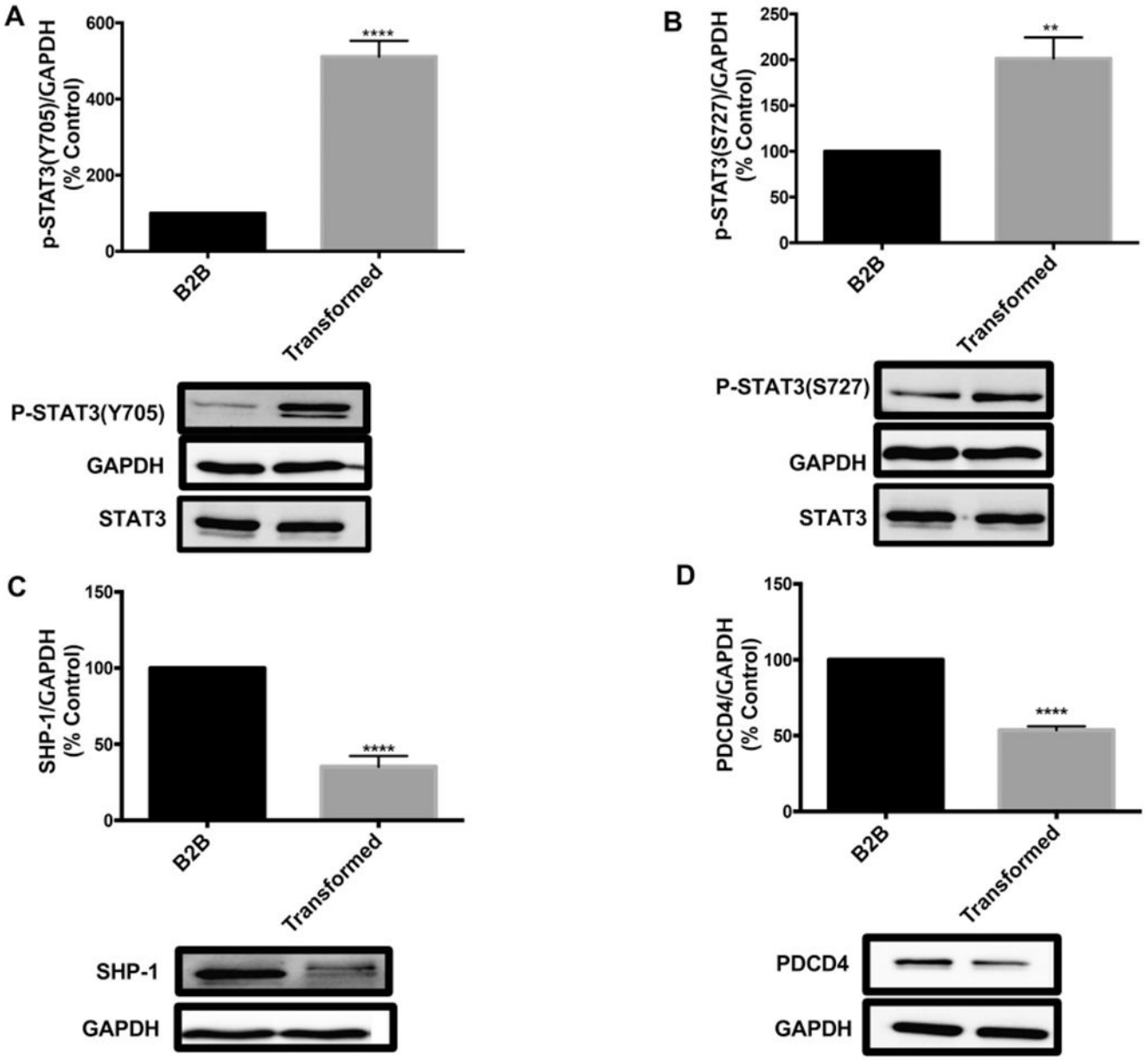

Fig. 6.

Increased protein levels of pSTAT3^{Y705} and pSTAT3^{S727} in transformed cells relative to the BEAS-2B cells. Cell lysates were prepared from both BEAS-2B cells and the As^{3+}-transformed cells for Western blotting using antibodies against pSTAT3^{Y705} (A), pSTAT3^{S727} (B), SHP-1 (C), and PDCD4 (D). Experiments were repeated three times, and the mean percent of protein/GAPDH ratio ± SEM was presented. One way ANOVA was used for statistics analysis. *:$p < 0.05$; **: $p < 0.01$; ***: $p < 0.001$, ****: $p < 0.0001$.

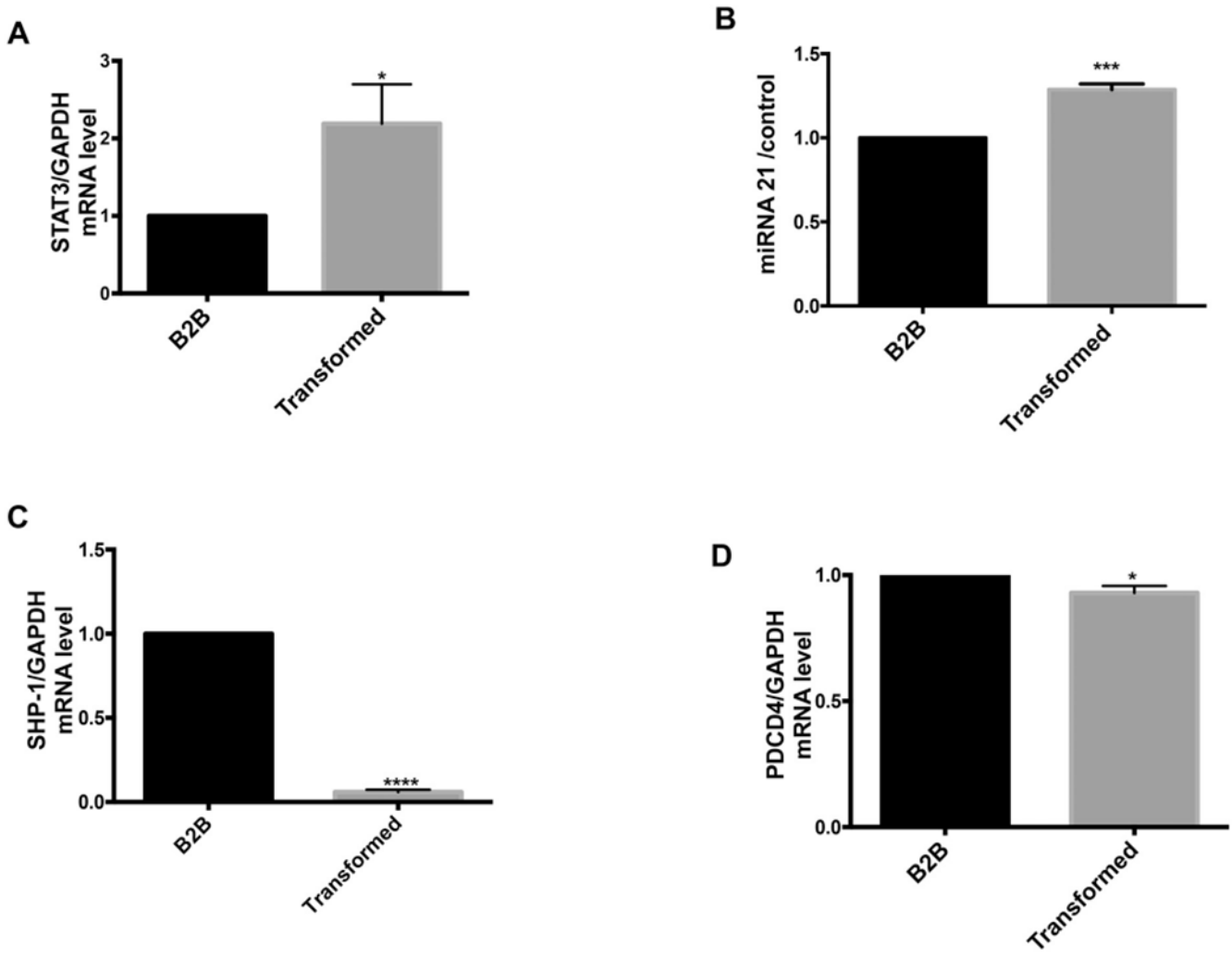

Fig. 7.

Increased mRNAs of STAT3 and miR-21, but decreased mRNAs of SHP-1 and PDCD4 in As^{3+}-transformed cells relative to the BEAS-2B cells. Total RNAs were prepared from the BEAS-2B cells and the transformed cells and subjected to QPCR for STAT3 (A), miR-21 (B), SHP-1 (C), and PDCD4 (D). Experiments were repeated three times, and the mean percent of mRNA/GAPDH mRNA ratio ± SEM was presented. One way ANOVA was used for statistics analysis. *:$p < 0.05$; **: $p < 0.01$; ***: $p < 0.001$, ****: $p < 0.0001$.

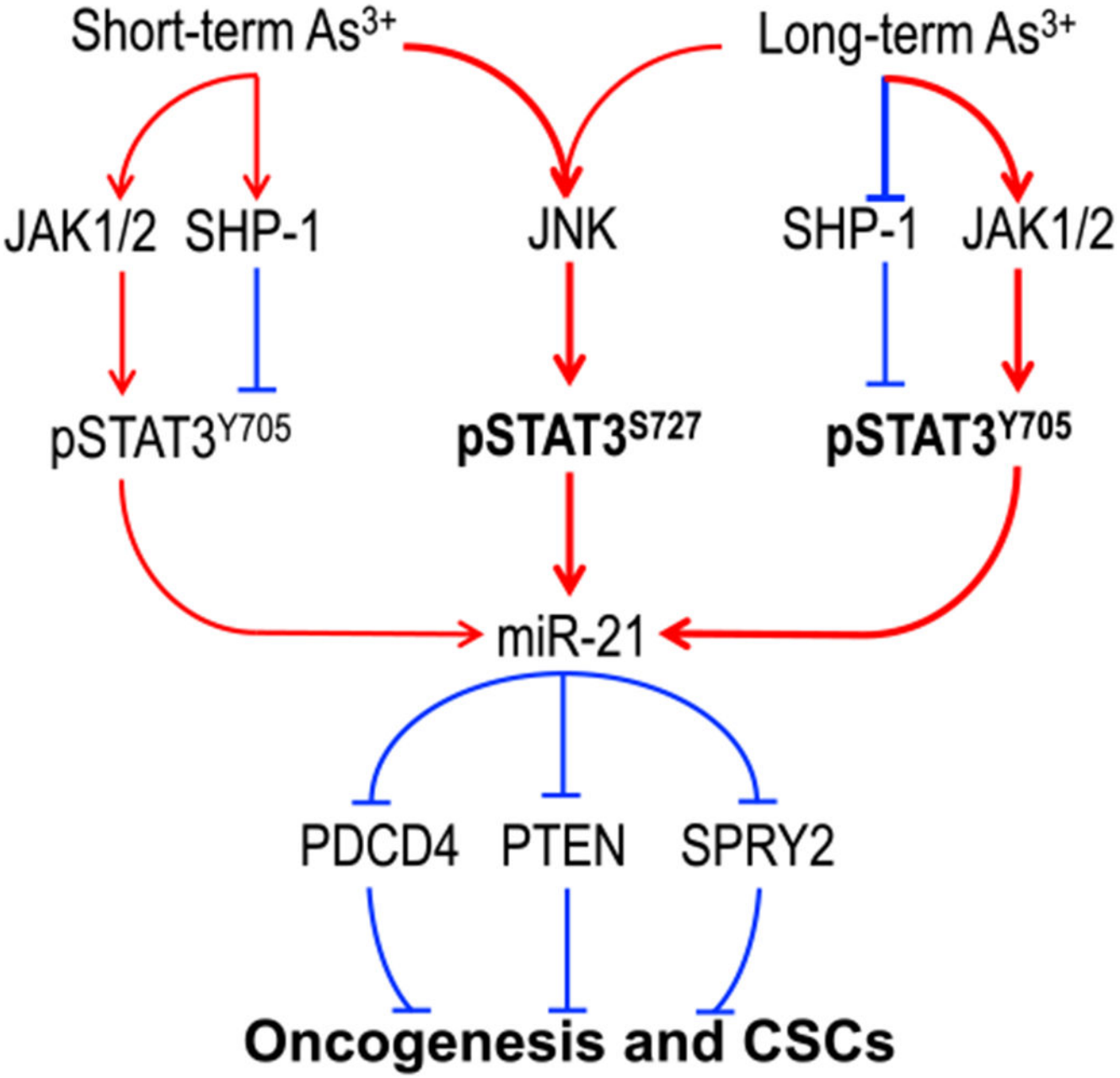

Fig. 8.

Diagram shows differences in the activation of STAT3 signaling between short-term and long-term As^{3+} treatment. In short-term treatment, As^{3+} activates JNK that linked to $pSTAT3^{S727}$ and stabilizes SHP-1 protein that down-regulates $pSTAT3^{Y705}$. In long-term treatment, due to the inhibition of SHP-1 at both the mRNA level and protein level, As^{3+} induces both $pSTAT3^{S727}$ and $pSTAT3^{Y705}$. One of the oncogenic activities of the activated STAT3, either $pSTAT3^{S727}$ or $pSTAT3^{Y705}$, or both, is achieved through the expression of an oncogenic non-coding RNA, miR-21 that negatively regulates several tumor suppressors,

such as PTEN, PDCD4 and SPRY2, leading to an enhanced oncogenesis and the generation of the CSCs.